Open Access Full Text Article

ORIGINAL RESEARCH

Carbon nanotube-based substrates promote cardiogenesis in brown adipose-derived stem cells via β1-integrin-dependent TGF-β1 signaling pathway

Hongyu Sun[1],*
Yongchao Mou[2],*
Yi Li[3],*
Xia Li[4],*
Zi Chen[2]
Kayla Duval[2]
Zhu Huang[1]
Ruiwu Dai[1]
Lijun Tang[1]
Fuzhou Tian[1]

[1]Department of General Surgery, Chengdu Military General Hospital, Chengdu, People's Republic of China; [2]Thayer School of Engineering, Dartmouth College, Hanover, NH, USA; [3]Department of Cardiology, The General Hospital of Chinese People's Armed Police Forces, Beijing, People's Republic of China; [4]Affiliated Hospital of Academy of Military Medical Sciences, Beijing, People's Republic of China

*These authors contributed equally to this work

Correspondence: Fuzhou Tian; Lijun Tang
Chengdu Military General Hospital, Chengdu, Sichuan Province 610083, People's Republic of China
Tel +86 28 8657 1251
Fax +86 28 8657 1251
Email tfz6689@163.com; tanglj@163.com

Abstract: Stem cell-based therapy remains one of the promising approaches for cardiac repair and regeneration. However, its applications are restricted by the limited efficacy of cardiac differentiation. To address this issue, we examined whether carbon nanotubes (CNTs) would provide an instructive extracellular microenvironment to facilitate cardiogenesis in brown adipose-derived stem cells (BASCs) and to elucidate the underlying signaling pathways. In this study, we systematically investigated a series of cellular responses of BASCs due to the incorporation of CNTs into collagen (CNT-Col) substrates that promoted cell adhesion, spreading, and growth. Moreover, we found that CNT-Col substrates remarkably improved the efficiency of BASCs cardiogenesis by using fluorescence staining and quantitative real-time reverse transcription-polymerase chain reaction. Critically, CNTs in the substrates accelerated the maturation of BASCs-derived cardiomyocytes. Furthermore, the underlying mechanism for promotion of BASCs cardiac differentiation by CNTs was determined by immunostaining, quantitative real-time reverse transcription-polymerase chain reaction, and Western blotting assay. It is notable that β1-integrin-dependent TGF-β1 signaling pathway modulates the facilitative effect of CNTs in cardiac differentiation of BASCs. Therefore, it is an efficient approach to regulate cardiac differentiation of BASCs by the incorporation of CNTs into the native matrix. Importantly, our findings can not only facilitate the mechanistic understanding of molecular events initiating cardiac differentiation in stem cells, but also offer a potentially safer source for cardiac regenerative medicine.

Keywords: carbon nanotube, brown adipose-derived stem cells, cardiomyocytes, TGF-β1, β1-integrin

Introduction

Ischemic cardiovascular diseases, such as myocardial infarction, lead to impaired cardiac output and cardiac performance as a result of the irreversible loss of contractile cardiomyocytes (CMs) and represent a leading cause of morbidity and mortality worldwide.[1,2] Stem cell-based therapy has emerged as a promising therapeutic alternative that is currently being explored as a means to repair the damaged myocardium.[3,4] Thus far, it has been shown that various populations of stem cells, such as bone marrow mesenchymal stem cells,[5] white adipose-derived stem cells,[6] umbilical cord blood stem cells,[7] and resident cardiac stem cells,[8] are capable of producing CMs to inhibit further deterioration and help restore cardiac function caused by ischemic heart disease. However, the differentiation ability of these stem cells into CMs was assisted by the stimulation of chemical inducers.[9]

Brown adipose-derived stem cells (BASCs) residing in the dorsal region are known to differentiate spontaneously into CMs without any chemical inducers in vitro.[10–12]

Because of this cardiomyogenic capability, BASCs, when transplanted into the infracted myocardium of rat models with myocardial infarction, integrate into the host heart and improve cardiac functions through differentiation into CMs, suggesting that BASCs remain an ideal cellular source for cardiac regenerative therapy.[10,11] Despite this outstanding spontaneous cardiogenesis, it remains crucial to find a simple, effective way to further increase stem cell cardiac differentiation for therapeutic applications.

Recently, nanomaterials possessing the unique features of the nanometer range (less than 100 nm) have gained significant interest for directing stem cell differentiation in stem cell-based regenerative medicine.[13,14] Carbon nanotubes (CNTs) are one of the major promising nanomaterials applied in the biomedical field due to their mechanical and electrical properties.[15,16] In terms of stem cell research, CNT substrates affect the morphogenesis and differentiation of multipotent adult stem cells due to their mechanical properties, nanoroughness, or conductivity. Tay et al[17] reported that human mesenchymal stem cells cultured on single-walled CNT films promoted cell adhesion, growth, and neural differentiation without the supplementation of a chemical inducer. Besides pure CNTs, various CNT-based composite materials composed of polymers or natural extracellular matrix, which endorses the composites with the unique properties, have been used for biomedical research. Poly(ε-caprolactone)-CNT composite scaffolds have been confirmed to enhance the adhesion and cardiac differentiation of human mesenchymal stem cells.[18] Numerous reports have shown that CNTs exert beneficial impacts on lineage specification of stem cells; nevertheless, the definite role of CNTs in regulation of cardiac differentiation of BASCs, and especially the underlying molecular mechanism, has not yet been revealed. Unveiling these events is a key step necessary for the application of CNTs in clinical scenarios for cardiac regeneration.

In our recent work,[19] we found that CNT-Col scaffolds exert facilitative effect on the electrical coupling of CMs. However, the effect of CNTs on cardiogenesis in BASCs and the maturation of these CMs derived from BASCs remain unclear. In this study, the potential effects of CNTs on different biophysical aspects of cardiogenesis in BASCs, including the morphological change, cell proliferation, and cardiac differentiation, were evaluated. Importantly, this study offers new insights into the underlying molecular requirements in the regulation of cardiogenesis and maturation of CMs derived from BASCs.

Material and methods
All Sprague Dawley rats were purchased from Chengdu Da Shuo Biotech Co., Ltd. (Chengdu, People's Republic of China). All experiments in this study were approved and in compliance with the guidelines of the Committee on the Ethics of Animal Experiments of Chengdu Military General Hospital, Chengdu, People's Republic of China.

Isolation, cultivation, and characterization of rat BASCs
BASCs were isolated from interscapular adipose tissues of Sprague Dawley rats (male, 80–100 g) as previously reported.[12] Briefly, the isolated brown adipose tissues were rinsed with phosphate-buffered saline (PBS), then minced with scissors, and finally digested with a mixture of 0.1% collagenase IV (Sigma-Aldrich, St Louis, MO, USA), 0.1% dispase II (Roche, Basel, Switzerland), and 0.05% trypsin (Gibco, Waltham, MA, USA) for 45 minutes at 37°C with gentle agitation. After digestion and filtering, cells were plated onto tissue culture dishes in α-MEM (Invitrogen, Carlsbad, CA, USA) culture medium containing 15% FBS (Invitrogen) at 37°C and 5% CO_2. For cell culture on the CNT-Col or Col substrates (10×10 mm), 2×10^5 BASCs were seeded, following the same procedure as cells on culture dishes.

To characterize the freshly isolated BASCs, 1×10^5 cells were stained with fluorescein isothiocyanate–conjugated anti-CD90, CD45, CD29, CD34, and CD133 antibodies and analyzed by flow cytometry (BD Biosciences, San Jose, CA, USA). The cardiomyogenic differentiation of BASCs was analyzed using immunofluorescence staining. The following cardiomyocyte-specific antibodies were used in our study: cardiac troponin T (cTnT), α-sarcomeric actinin (α-SA), GATA-4, Nkx2.5, and connexin 43 (Cx43). Each experiment was repeated at least three times.

Preparation and characterization of CNT-Col composite scaffolds
CNT-Col composite scaffolds were fabricated and characterized as previously described.[19] In brief, single-walled CNTs (0.7–1.2 nm in diameter and 100–1,000 nm in length, 95% purity; Nanostructured & Amorphous Materials, Inc., Houston, TX, USA) were functionalized with a collagen I solution using the noncovalent method. Then, the CNT-Col composites with a final concentration of 0.1 mg/mL CNTs were deposited onto glass coverslips (10×10 mm) with a high enough volume to obtain CNT-Col substrates. Pure Col substrates were also used as control. The characteristics of

CNT-Col composite scaffolds, including the surface topography, electrical conductivity, and the surface roughness, were examined by scanning electron microscopy (SEM), an HP 34401A multimeter, and atomic force microscope as previously described, respectively.[19]

Measurement of cell adhesion and elongation

To assess the morphological variation of BASCs induced by the substrates, we performed fluorescence staining of F-actin. In brief, after 1 and 3 days of incubation at 37°C and 5% CO_2, the engineered constructs of cells and scaffolds were fixed using 4% paraformaldehyde for 30 minutes at room temperature, and then stained with fluorescein isothiocyanate–conjugated phalloidin (1:500; Invitrogen) for F-actin and 4,6-diamidino-2-phenylindole (1:1,000; Molecular Probes, MA, USA) for the cell nucleus. The results were observed by confocal microscopy. To determine the potential effects of CNTs on cell adhesion of BASCs, ten pictures per section under $20 \times$ fields of BASCs on CNT-Col or Col substrates were randomly acquired for analysis using ImageJ software (National Institute of Health). Additionally, to quantify the cell shape change due to the incorporation of CNTs, the cell area and the long/short axis of BASCs at days 1 and 3 were analyzed with ImageJ software. An average of 300 cells was counted for each sample group.

Alamar Blue assay

The impact of CNTs on cell viability in the cell-scaffold constructs was evaluated using Alamar Blue assay. Over 1 and 3 days' cultivation period, the cell-scaffold constructs were incubated for 6 hours with Alamar Blue reagent. The supernatant was determined by spectrophotometry at 570 and 600 nm using a CytoFluor™ 2300 (Millipore, Billerica, MA, USA) plate reader. Independent experiments were conducted three times for each group.

Quantitative real-time reverse transcription-polymerase chain reaction

Total RNA from BASCs on CNT-Col or Col substrates for 1, 3, 7, and 10 days was extracted using Trizol reagent (Invitrogen) according to the manufacturer's instructions. Then, 1 µg of RNA was used to synthesize cDNA with M-MLV RT First-Strand cDNA Synthesis Kit (Invitrogen). For quantitative real-time reverse transcription-polymerase chain reaction (qRT-PCR), the primers for NKX2.5, GATA-binding protein 4 (GATA-4), Tbx5, α-MHC, β-MHC, cTnT,

and GAPDH (Table S1) were used, with GAPDH as control. For qRT-PCR, the reaction mixture began with 5 minutes at 95°C to activate TaqDNA polymerase followed by 35 cycles of 15 seconds at 95°C, 45 seconds at 57°C, and later followed by extension at 72°C for 60 seconds. For each gene, the data were analyzed using the comparative Ct method ($2^{-\Delta\Delta Ct}$). In all cases, each PCR was repeated in triplicate with at least three independent experiments.

Immunofluorescence staining and confocal microscopy

For immunofluorescence staining, the cell-scaffold constructs were fixed in 4% formaldehyde for 30 minutes at room temperature, permeabilized with 0.3% Triton X-100 in PBS for 10 minutes, and then blocked with 2% BSA, 0.05% sodium azide in PBS for 45 minutes to block nonspecific antibody binding. Subsequently, constructs were incubated with the primary antibodies overnight at 4°C. The primary antibodies used were as follows: rabbit monoclonal anti-Troponin I (1:100; AbCam, Cambridge, MA, USA), and mouse monoclonal anti-α-SA (1:100; AbCam), rabbit polyclonal anti-connexin-43 (1:1,000; AbCam), rabbit polyclonal anti-GATA-4 (1:100; Santa Cruz, CA, USA) and rabbit polyclonal anti-Nkx2.5 (1:200; Santa Cruz, CA, USA). Constructs were then washed three times for 10 minutes with PBS and incubated with Alexa Fluor 488- or Alexa Fluor 548-conjugated secondary antibodies (1:500; Invitrogen) for 1 hour in the dark at room temperature. Confocal images were acquired using a Zeiss LSM 510 microscope. Immunofluorescent staining was also performed to assess cell proliferation on the scaffolds. On days 1 and 3 of culture, the cell-scaffold constructs were stained with antibodies against proliferating cell nuclear antigen (PCNA; 1:200; Abcam). Twenty different images were randomly captured for each group, and the PCNA-positive cells were quantified using ImageJ software.

Assay of sarcomere length and Z-line width

The sarcomere length was assessed by measuring the distance between α-SA-stained Z-line structures from α-SA+ cells with visible sarcomere structures as previously reported.[20] Different striation regions of ten cells were calculated using ImageJ software. Z-line width was also assessed using ImageJ software according to a previous study,[21] and ten α-SA+ cells were measured with ten measurements for each cell.

Transmission electron microscopy analysis of BASCs grown on CNT-Col substrates

The samples were fixed in a 2.5% solution of glutaraldehyde in 0.1 M sodium cacodylate buffer (pH =7.4) for 6 hours, postfixed in 1% phosphate-buffered OsO_4 for 2 hours, and embedded in epoxy resin. Semithin sections were obtained with an LKB NOVA ultramicrotome, then stained with toluidine blue in 0.1 M borate buffer, and finally observed under a light microscope. Ultrathin sections of the areas of interest were sliced and examined by a transmission electron microscope (Technai10; Philip, Einhoven, the Netherlands) at accelerating voltage about 150 kV.

TGF-β1 bioassay

TGF-β1 levels in BASCs grown on the scaffolds were quantified using a commercially available ELISA kit (TGF-β1 Emax® ImmunoAssay System; Promega, Madison, WI, USA) according to the protocol provided by the manufacturer. For each sample, TGF-β1 measurements were made twice. The data were expressed as a mean value ± SD of three independent experiments.

Protein isolation and Western blot analysis

Western blot assays were performed as described previously.[18] In brief, the total protein of the cell-scaffold constructs was prepared using lysis buffer (Tiandz, Beijing, People's Republic of China). For determination of Western blotting by SDS-PAGE, 100 μg total protein was separated by SDS-PAGE electrophoresis, and anti-α-SA (Abcam), anti-β1-integrin (Abcam), anti-phospho-Smad 2 (Cell Signaling Technology, Beverly, MA, USA), and anti-Smad 2 antibodies (Cell Signaling Technology) were used to incubate the polyvinylidene difluoride membrane with total protein. Enhanced chemiluminescence reagent (Amersham, MA, USA) was utilized to detect the labeled proteins. In some experiments, BASCs grown on the scaffolds were incubated in serum-free medium containing anti-β1-integrin antibody (clone Ha2/5; BD Pharmingen, CA, USA) for 1 hour in 37°C, 0.05% CO_2 to block signaling mediated by β1-integrin, which was shown by previous studies.[22] Then, the treated constructs were cultured in normal medium for 7 days. In some other experiments, constructs were incubated with ALK-specific inhibitor, SB431542 (10 μM), for 7 days. The band intensities were analyzed with the ImageJ software.

Statistical analysis

Data were expressed as mean ± standard error of the mean. The unpaired two-tailed Student's *t*-test was used to analyze differences between two groups. Group differences were conducted by one-way analysis of variance with Tukey's post hoc test. *P*-values <0.05 were considered statistically significant (**P*<0.05, ***P*<0.01, ****P*<0.001). All statistical analyses were performed with SAS statistical software version 9.1 (Cary, NC, USA).

Results
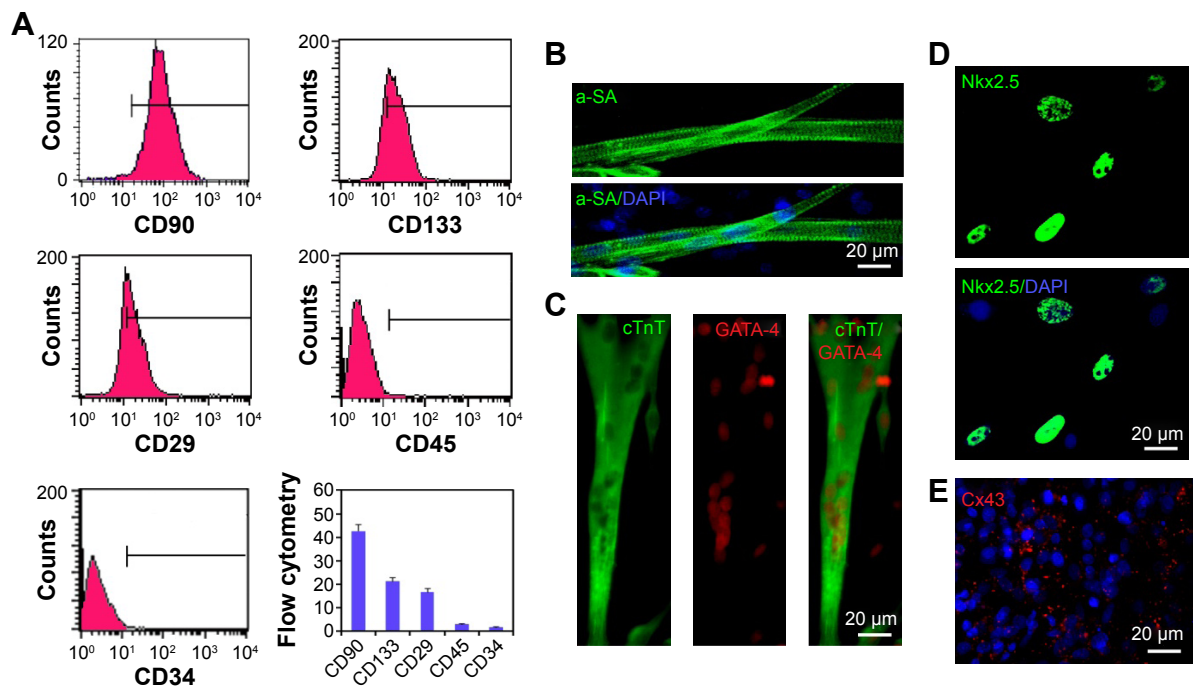## Cultivation and characterization of rat BASCs

Previous studies indicated that there existed multiple surface antigenic markers, such as CD90, CD133, and CD29 in BASCs, which have the spontaneous capability of cardiogenesis. The collected cells from brown adipose tissues were characterized through fluorescence-activated cell sorting analysis (Figure 1A). The population of BASCs was positive for CD90, CD133, and CD29, but negative for CD45, a hematopoietic and leukocyte marker. Among them, it is rather remarkable that the population of CD133-positive cells with a percentage of ~20% were reported to have a high efficiency of cardiogenesis.

BASCs with an elongated phenotype began to contract spontaneously within 1 week after isolation. Increasingly more BASCs with synchronous contraction became significantly elongated over the time course of the experiment. To further illustrate the cardiomyogenic differentiation of BASCs, we performed immunofluorescence staining against cardiac-specific markers (Figure 1B and C). The elongated cells with clear transverse striation positively expressed cTnT and α-SA at day 21 in culture. In addition, the cardiac-specific transcription factors GATA-4 and Nkx2.5 were expressed in the cell nuclei distinctively (Figure 1C and D). Furthermore, gap junctions formed at the intercellular sites where Cx43 was found (Figure 1E). Therefore, the isolated BASCs had the capability to spontaneously differentiate into CMs.
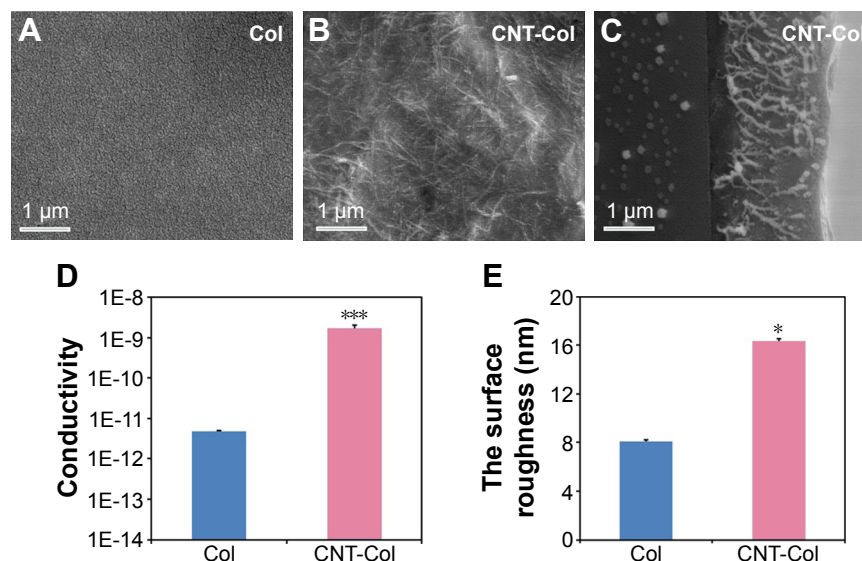
Characteristics of CNT-Col composite substrates

CNT-Col composite scaffolds were fabricated and characterized as previously described.[19] In particular, the CNT-Col scaffolds were prepared by coating of 0.1 mg/mL single-walled CNTs on bare glass coverslips, which were modified with collagen I matrix using noncovalent method.

SEM observation demonstrated a continuous network with CNT bundles uniformly distributed in the collagen matrix (Figure 2A and B). SEM sagittal images showed that the thickness of CNT-Col scaffolds was about 2.29 μm (Figure 2C). Generally, the conductivity of CNT-Col scaffolds was

Figure 1 Phenotype and cardiac differentiation of rat BASCs.
Notes: (**A**) FACS analysis for surface markers of the isolated BASCs. These cells expressed CD90, CD133, and CD29 and but did not express CD45, a hematopoietic and leukocyte marker. (**B–E**) Immunofluorescence staining of cardiomyocyte-specific markers, including sarcomeric actin (α-SA, green) (**B**), double-stained for cTnT (green)/ GATA-4 (red) (**C**), Nkx2.5 (green) (**D**), Cx43 (red) (**E**), indicated BASCs expressed cardiac transcription factors GATA-4 and Nkx2.5 and had the capacity to differentiate into cardiomyocytes. Cell nuclei were stained with DAPI (blue). Data are means $\pm$ SEM. All experiments were performed in triplicate.
Abbreviations: FACS, fluorescence-activated cell sorting; BASCs, brown adipose-derived stem cells; DAPI, 4,6-diamidino-2-phenylindole.

observed to be significantly higher in comparison to the pure collagen substrates (Figure 2D). Furthermore, the surface roughness of CNT-Col scaffolds was significantly greater compared to Col scaffolds (as measured by atomic force microscope analysis; Figure 2E). These results indicated that the addition of CNTs into the collagen scaffold increased the electrical conductivity and the surface roughness.

Figure 2 Characteristics of CNT-Col composite substrates.
Notes: (**A**) Representative SEM images of Col scaffolds. (**B**) SEM observation demonstrated a continuous network with CNT bundles uniformly distributed in the collagen matrix. (**C**) SEM sagittal images showed that the thickness of CNT-Col scaffolds was about 2.29 μm. (**D**) The conductivity of CNT-Col scaffolds was observed to be significantly higher in comparison to the pure collagen substrates. (**E**) The surface roughness of CNT-Col scaffolds was significantly greater compared to Col scaffolds, as measured by atomic force microscopy analysis. Data are means $\pm$ standard error of the mean. *$P<0.05$, ***$P<0.001$. All experiments were performed in triplicate.
**Abbreviations:** Col, collagen; CNT, carbon nanotube; SEM, scanning electron microscopy.

CNTs supported BASCs morphology and proliferation

To begin to evaluate CNTs contributions to the cell adhesion of BASCs, we visualized the cells attaching to substrates using F-actin. With the staining of F-actin, the structural changes of BASCs at days 1 and 3 were visualized clearly in consequence of the addition of CNTs. Notably, BASCs on CNT-Col substrates appeared more stretched and formed thicker actin filaments compared to those on Col substrates (Figure 3A). To quantify the correlation of CNTs and the cellular adhesion of BASCs, we sought to analyze the area of individual cells, the cell number per field, and the long/short axis length using ImageJ software. The results revealed that CNT-Col substrates increased the adherent area of individual BASCs and the number of adherent cells significantly, compared to those on Col substrates (Figure 3B). Meanwhile, the ratio of long and short axial lengths of the BASCs on CNT-Col substrates appeared smaller than those on Col substrates (Figure 3C and D).

To assess whether the addition of CNTs affected cell viability, we measured the metabolic activity of BASCs through the Alamar Blue-based assay (Figure 3E). The relative number of live cells in culture for 24 hours in the two groups, which was notably uncorrelated with the incorporation of CNTs in substrates, increased in culture for 72 hours on CNT-Col substrates more than those on Col substrates (Figure 3E). Furthermore, the proliferative capacity of BASCs was promoted by CNTs, as shown by the staining of PCNA (Figure 3F and G). Additionally, the amount of caspase-3, as a cysteine protease involved in apoptosis, was markedly reduced on the CNT-Col substrates compared to control (Figure 3H). Therefore, CNT-Col substrate appeared to be superior to the pure collagen matrix and supported BASCs remarkably in terms of cell adhesion, spreading, viability, and proliferation.
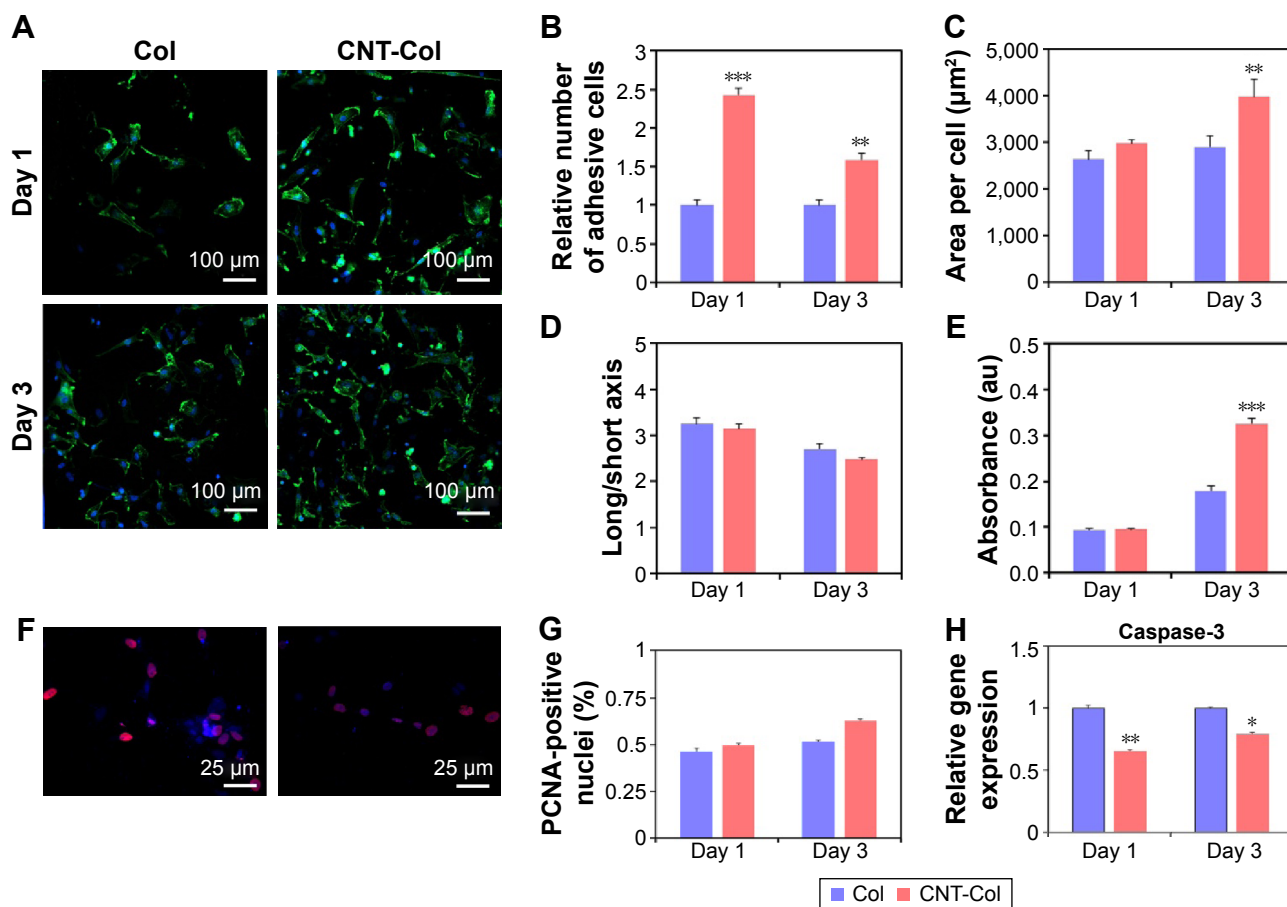
Figure 3 Morphology and proliferation of BASCs grown on CNT-Col substrates and Col substrates.
Notes: (**A**) Fluorescence staining of F-actin showing that BASCs adhered on CNT-Col substrates spread wider, and their actin filaments looked thicker compared to those on Col substrates. (**B**–**D**) Graphs showing the percentage cell adhesion (**B**), the area of individual cells (**C**), and the long/short axis (**D**) on CNT-Col substrates were significantly higher than those on pristine collagen at days 1 and 3. (**E**) The averaged value of Alamar Blue-based assay at days 1 and 3. (**F** and **G**) PCNA staining indicating that the proliferative capacity of BASCs on CNTs was higher than on Col substrates. (**H**) Cell viability of BASCs grown on the two substrates at days 1 and 3. Data are means ± standard error of the mean. *Significant difference when compared to control group, *$P<0.05$, **$P<0.01$, ***$P<0.001$. All experiments were performed in triplicate.
Abbreviations: CNT, carbon nanotube; Col, collagen; BASCs, brown adipose-derived stem cells; PCNA, proliferating cell nuclear antigen; SEM, standard error of mean.

CNTs accelerated cardiogenesis in BASCs

The cardiac specific proteins, α-SA and Cx43, were examined by immunofluorescent staining to assess the potential effect of CNTs on cardiogenesis in BASCs cultured for 3, 7, and 10 days.

BASCs grown on the CNT-Col substrates exhibited an elongated rod shape and beat spontaneously for up to 3 days after isolation. This visible contractile activity was used to address the critical issues of our study: whether the cardiogenesis in BASCs was accelerated by substrates containing CNTs. There were several α-SA+ cells on the CNT-Col substrates, while only sporadic α-SA+ cells were on the control group (Figure 4A). Noticeably, the percentage of α-SA+ cells was significantly higher on CNT-Col substrates than those on Col substrates (Figure 4B).

At day 7, there were more aligned α-SA+ cells with an elongated phenotype of the CNT-Col substrates. The significant increase in the contraction rates as well as the amplitude

of contraction of cells on CNT-Col substrates was shown to be time dependent (Figure 4A, Videos S1 and S2). Furthermore, α-SA+ cells on the CNT-Col substrates had an abundance of better-organized myofilaments, which is a hallmark of mature CMs (Figure 4A). In contrast, the number of α-SA+ cells with spontaneous contractile activity on Col substrates was fewer, and also the number of sarcomeres in cells on the Col substrates was lower relative to cells on CNT-Col substrates.

After culture of 10 days, the elongated and contractile CMs, derived from BASCs, assembled into typical bundles with uniform contraction, forming clear visible myotubes (a feature crucial to cardiac contractile function) on CNT-Col substrates, compared to the significant variation seen on Col substrates. In addition, α-SA+ cells on a CNT-Col matrix possessed better aligned registers of sarcomeres, which increased significantly by day 10 (Figure 4A and B). Furthermore, considering that sarcomeres are effective indicators of twitch power generated by CMs, the sarcomere length and Z-line width were determined. As shown in Figure 4C and D,
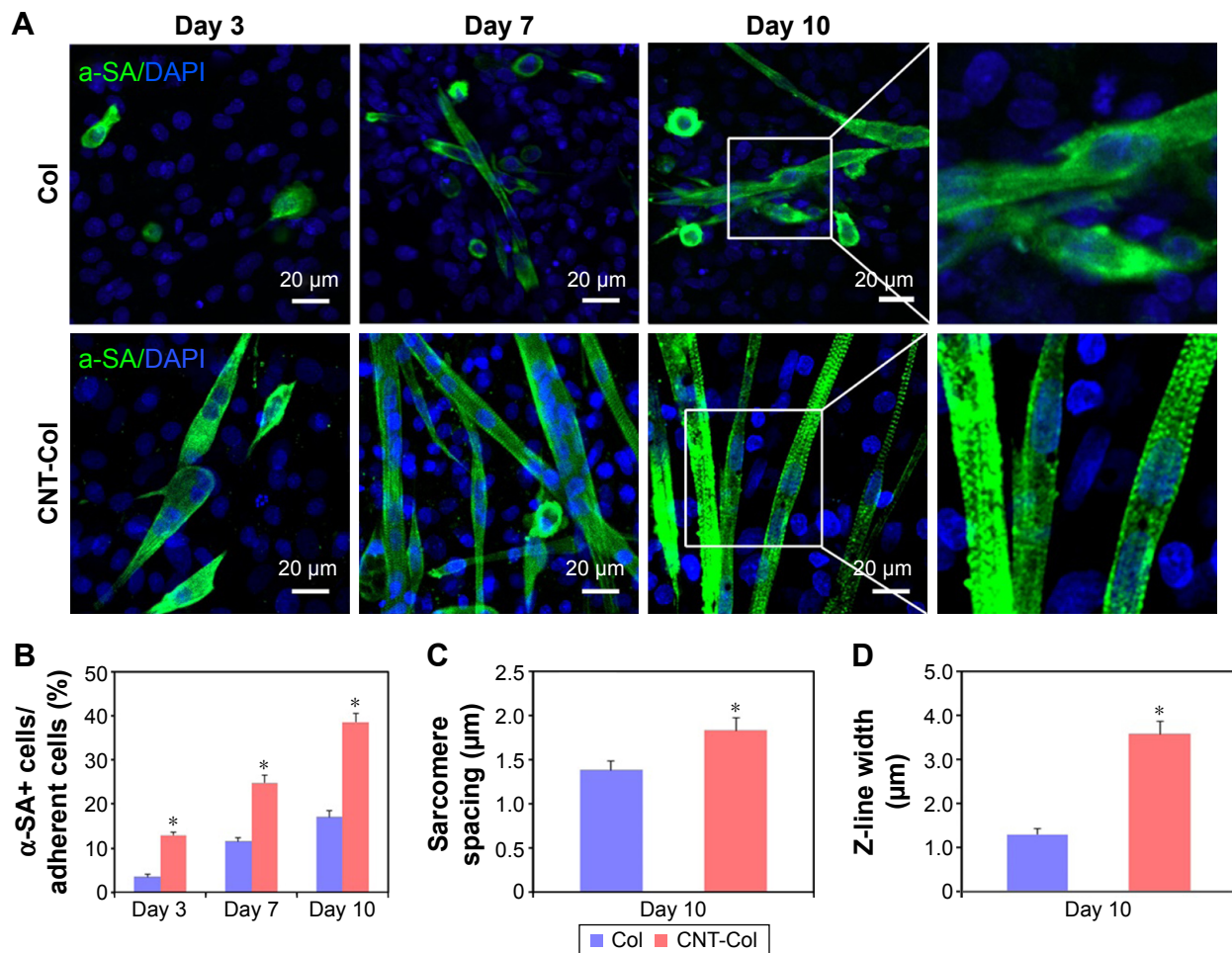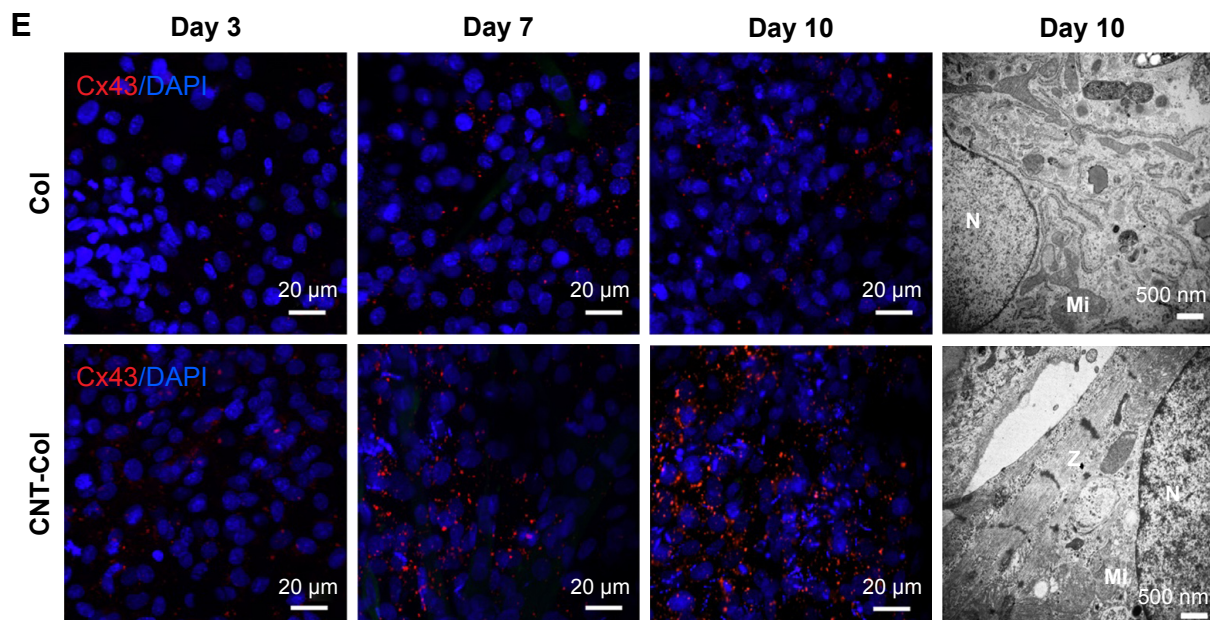

Figure 4 (*Continued*)

Figure 4 CNTs accelerated cardiogenesis in BASCs and the maturation of BASC-cardiomyocytes (BASC-CMs).
Notes: (**A**) Immunofluorescent staining of α-SA showing BASCs grown on CNT-Col substrates and Col substrates at days 3, 7, and 10. (**B**) The percentage of α-SA+ cells of total adherent cells on the two substrates was counted at days 3, 7, and 10. (**C**) Sarcomere length had significant improvement in BASCs grown on CNT-Col substrates in comparison to those on Col matrix; n=10 cells per group. (**D**) Z-line width measurements showed there was significant improvement in BASCs grown on CNT-Col substrates when compared to those on Col matrix; n=10 cells per group. (**E**) Immunofluorescent staining of gap junction protein Cx43 showing BASCs grown on CNT-Col substrates and Col substrates at days 3, 7, and 10. (**F**) Electron microscopy observation showed BASCs on the CNT-Col substrates possessed better organized cross-striated myofilaments. Z: Z-line; N: nucleus; Mi: mitochondrion. Data are means ± SEM. *Significant difference when compared to control group, *$P<0.05$. All experiments were performed in triplicate.
Abbreviations: CNT, carbon nanotube; Col, collagen; BASCs, brown adipose-derived stem cells; SEM, standard error of mean; DAPI, 4,6-diamidino-2-phenylindole; N, nucleus; Mi, mitochondrion.

BASC-CMs on CNT-Col matrices showed significant increase in both sarcomere length and Z-line width when compared to those on Col matrices.

In addition, Cx43, a main component of gap junctions, was scattered throughout the cytoplasm and cytomembrane of BASCs for both groups. An increased accumulation of Cx43 was observed in the intercellular sites of neighboring BASCs on CNT-Col substrates compared to the control group (Figure 4E). This increase suggests an appearance of gap junctions and electric coupling between neighboring CMs.

Overall, the incorporation of CNTs into the matrix promoted the cardiac differentiation efficacy of BASCs and accelerated the maturation of BASC-CMs, which is consistent with our expectations.

CNT-Col substrates induced the cardiomyogenic expression of BASCs

To quantify the underlying effects of CNTs on cardiogenesis in stem cells, we then analyzed the expression of heart-specific markers in BASCs on the CNT-Col substrates, spontaneously, without any inducers for cardiomyogenic differentiation.

Notably, the gene expression of representative markers for cardiomyogenic differentiation, including Nkx2.5, GATA-4, Mef2c, α-MHC, β-MHC, and cTnT, was enhanced in BASCs

on the CNT-Col substrates when compared to those on the Col substrates, although the level of increase was different (Figure 5). Nkx2.5, GATA-4, and Tbx5, which are the main cardiac transcription factors of stem cells, were remarkably upregulated in BASCs on the CNT-Col substrates (Figure 5A–C). However, there was a clear decrease in the expression of these transcription factors over time. Between days 3 and 10 of cell culture, the presence of CNTs in the substrate induced the expression of standard cardiomyogenic contractile proteins significantly, such as α-MHC, β-MHC, and cTnT. Nevertheless, α-MHC and β-MHC, which are the markers for early CMs, reached the maximum expression in BASCs on day 7, and then decreased on day 10 in the CNT-Col group, whereas cTnT as the marker for mature CMs followed an increasing trend during culture from day 3 to day 10 (Figure 5D–F). These data further suggested that CNTs were a major contributing factor in the differentiation of BASCs into CMs, and agreed well with the previous results from immunofluorescence staining.

TGF-β1 signaling pathway plays a pivotal role in CNT-promoted cardiogenesis in BASCs

Several signaling pathways have been demonstrated to play crucial roles in the cardiac differentiation of stem cells,
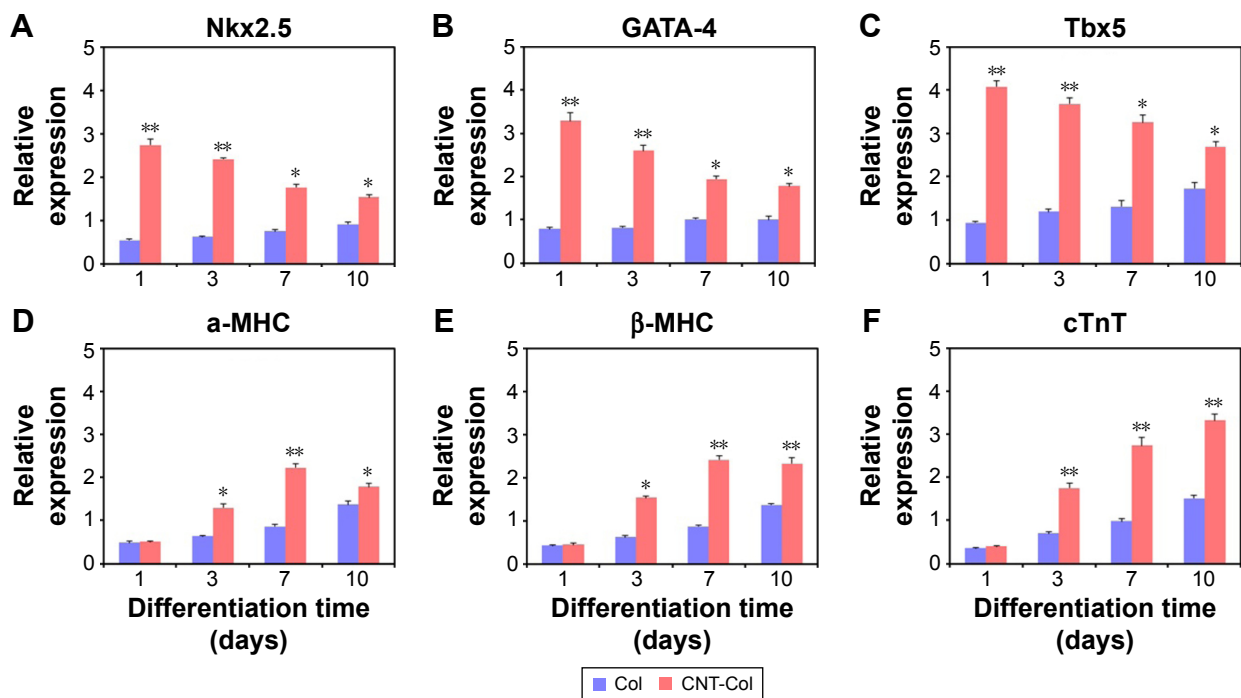
Figure 5 Cardiac gene expressions of BASCs cultured on CNT-Col substrates and Col substrates for 3, 7, and 10 days, including Nkx2.5 (**A**), GATA-4 (**B**), Tbx5 (**C**), α-MHC (**D**), β-MHC (**E**), and cTnT (**F**).
Notes: Data are means ± SEM. *Significant difference when compared to control group, *$P<0.05$, **$P<0.01$. All experiments were performed in triplicate.
Abbreviations: Col, collagen; CNT, carbon nanotube; BASCs, brown adipose-derived stem cells; SEM, standard error of mean.

including TGF-β1, BMP6, and Wnt signaling pathways.[23–25] To assess the potential contribution of TGF-β1 signaling pathways to the activation of BASC cardiogenesis by CNTs, we analyzed the secretion of TGF-β1 through ELISA assay and Western blotting.

Interestingly, the TGF-β1 signaling pathway was activated to regulate the CNT-promoted cardiac differentiation of BASCs (Figure 6). The total levels of TGF-β1 in BASCs cultured on CNT-Col substrates were similar and only moderately higher than those on Col substrates on days 3 and 7 (Figure 6A). Moreover, the release of active TGF-β1 showed an approximate twofold and threefold increase in BASCs on CNT-Col substrates than those in the control group on days 3 and 7, respectively (Figure 6B). Furthermore, we determined whether the supplement of CNTs in substrates was capable of activating the TGF-β1 signaling by examining the phosphorylation of Smad. The results indicate that there was a remarkable promotion of TGF-β1-induced Smad2 phosphorylation in BASCs grown on CNT-Col matrices compared to the control group (Figure 6C and D), indicating that the facilitative effect of CNTs on cardiac differentiation of BASCs might be attributed to the activation of TGF-β1 signaling. To further examine this conjecture, an ALK5 kinase inhibitor, SB431542, was added into the culture medium to block TGF-β1 signaling on CNT-Col-based constructs.

The results showed that SB431542 inhibited the differentiation of BASCs into CMs significantly as demonstrated by a-actinin expression (Figure 6E and F).

β1-integrin-dependent TGF-β1 signaling is required for the CNT-promoted cardiac differentiation of BASCs

Previous results have shown that the incorporation of CNTs in natural matrix can improve the mechanical properties of composite biomaterials.[26–28] Given that β-integrin, known as a mechanotransducer, can regulate TGF-β1 signaling pathway,[29] we then investigated whether β-integrin was involved in the promotion of cardiac differentiation of BASCs due to CNT incorporation through the TGF-β1 pathway.

First, the expression of activated β1-integrin in BASCs cultured on CNT-Col scaffolds was twofold higher than those cultured on Col scaffolds at day 7, while all β1-integrin remained roughly constant in these two groups (Figure 7A–C). These results suggest that the β1-integrin signaling was activated in BASCs by the presence of CNTs, and thus, this might be involved in the regulation of CNT-promoted cardiogenesis in BASCs.

Next, to confirm the role of β1-integrin in the promotion of BASC cardiogenesis due to CNTs, the BASCs grown on CNT-Col substrates were incubated with anti-β1-integrin
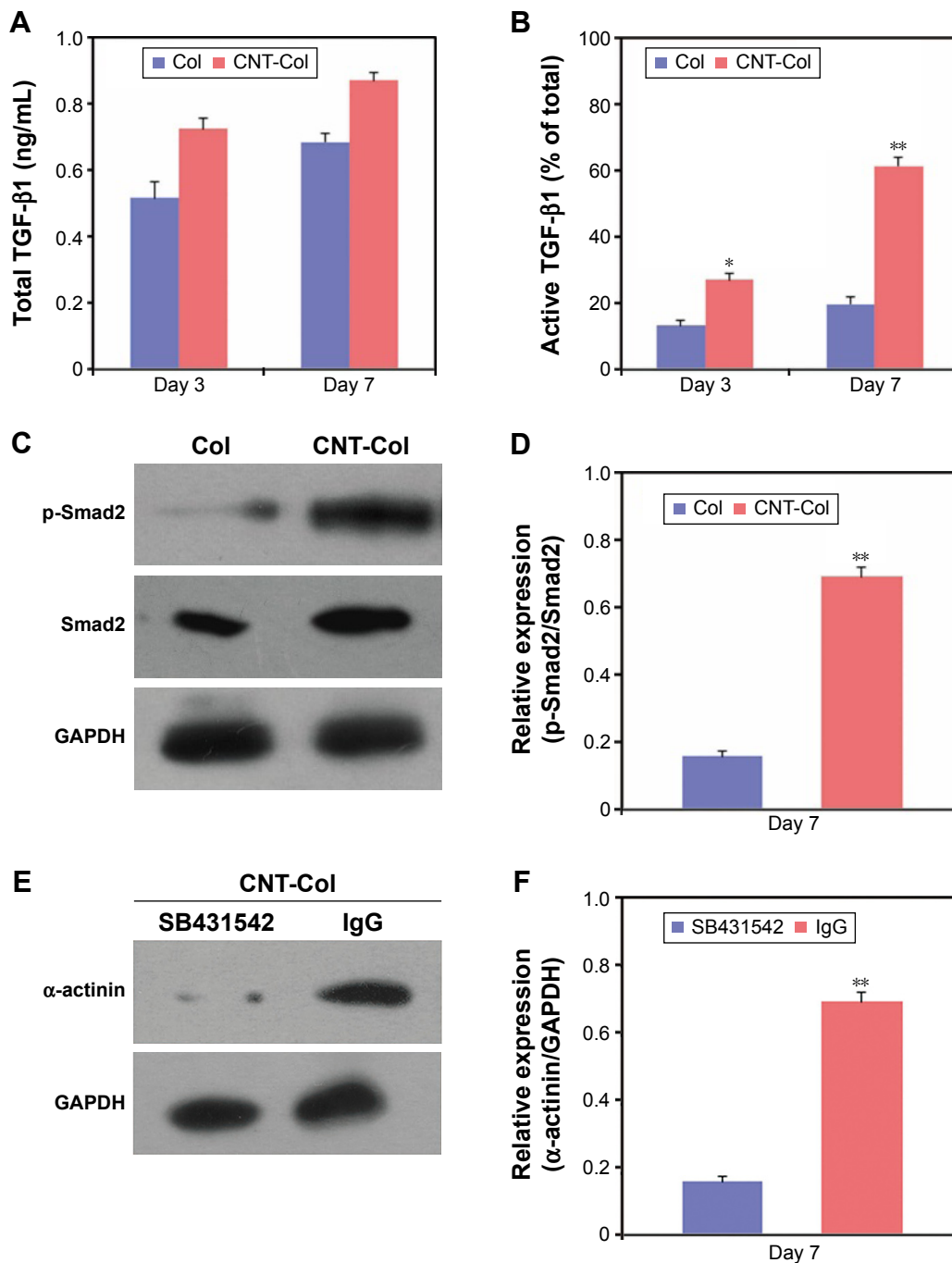
A

B

C

D

E

F

Figure 6 TGF-β1 signaling pathway plays a pivotal role in CNT-promoted cardiogenesis in BASCs.
Notes: (**A**) The amount of the total TGF-β1 in BASCs grown on CNT-Col substrates and Col substrates at days 3 and 7. (**B**) Quantification of the active TGF-β1 released in BASCs grown on CNT-Col substrates and Col substrates at days 3 and 7. The results were measured as a percentage of total TGF-β1. (**C**) and (**D**) Western blot showed BASCs grown on CNT-Col showed a remarkable increase in TGF-β1-induced Smad2 phosphorylation when compared with the control group at day 7. (**E**) and (**F**) Western blot showed the markedly elevated expression of β1-integrin in cultured BASCs on CNT-Col substrates compared to those on Col substrates at day 7. Data are means ± SEM. *Significant difference when compared to control group, *$P<0.05$, **$P<0.01$. All experiments were performed in triplicate.
Abbreviations: CNT, carbon nanotube; Col, collagen; BASCs, brown adipose-derived stem cells; SEM, standard error of mean.

function-blocking antibodies to inhibit the activation of β1-integrin. As shown in Figure 7D and E, the anti-β1-integrin antibody (ITG Ab) blocked the increase of α-actinin in the CNT-Col group, while no apparent changes of α-actinin were observed in BASCs grown in the control group. Most importantly, blocking of β1-integrin in CNT-Col scaffold-based constructs significantly induced the decrease of α-MHC and active TGF-β1 levels on days 3 and 7 (Figure 7F–H). Taken together, these results suggest that β1-integrin-mediated TGF-β1 signaling pathway is
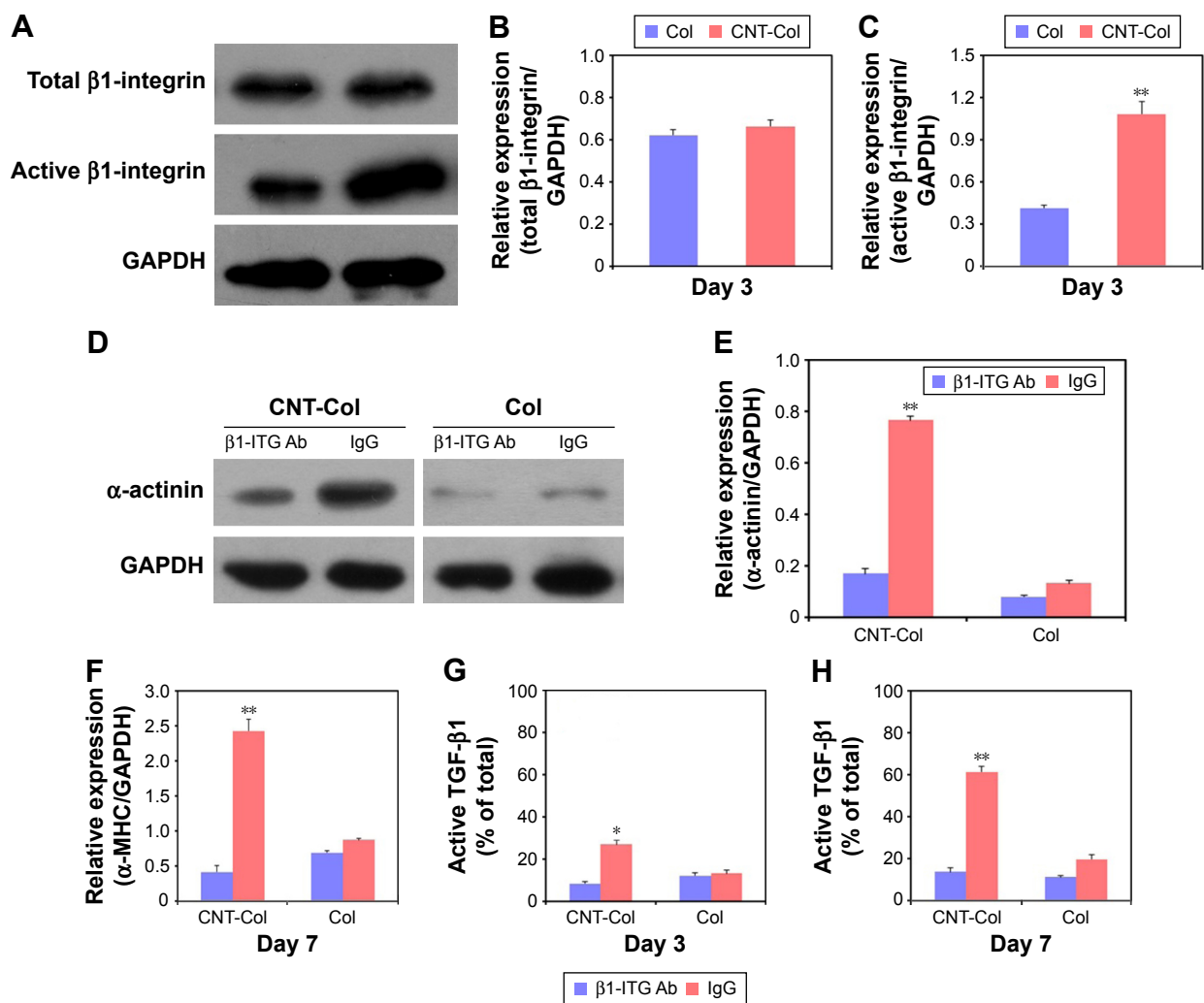
Figure 7 β1-integrin-dependent TGF-β1 signaling is required for the CNT-promoted cardiac differentiation of BASCs.
Notes: (**A**–**C**) Western blot showed activated β1-integrin protein expression in BASCs cultured on CNT-Col scaffolds was twofold higher than those cultured on Col scaffolds at day 7, while all β1-integrin remained roughly constant in these two groups. (**D** and **E**) Western blotting revealed the anti-β1-integrin antibody blocked the increase of α-actinin in the CNT-Col group, while no apparent changes of α-actinin showed in BASCs grown in the control group. (**F**–**H**) Blocking of β1-integrin signaling in CNT-Col scaffold-based constructs significantly induced the decrease of active TGF-β1 levels on days 3 and 7. Data are means ± SEM. *Significant difference when compared to control group, *$P<0.05$, **$P<0.01$. All experiments were performed in triplicate.
Abbreviations: CNT, carbon nanotube; Col, collagen; BASCs, brown adipose-derived stem cells; SEM, standard error of mean.

required for the facilitative effect of CNTs on cardiac differentiation of BASCs.
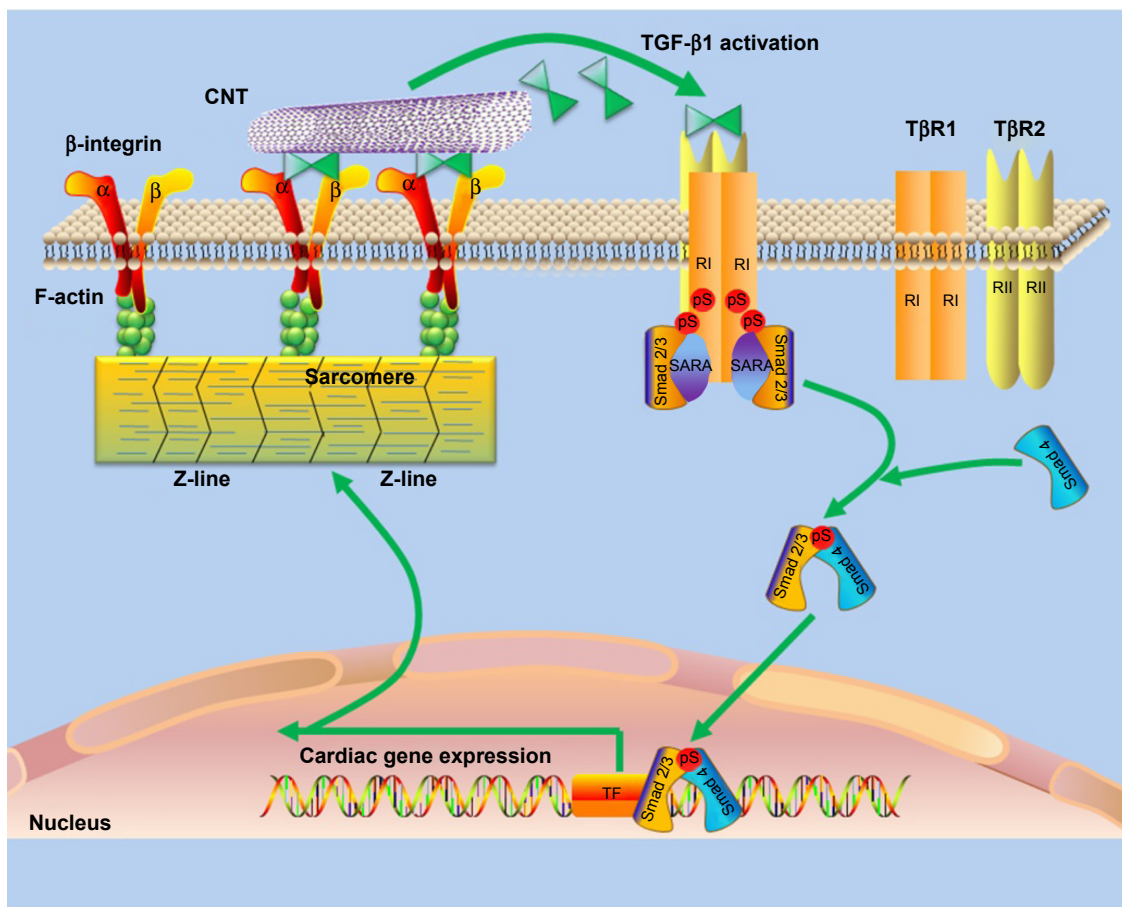
Last but not least, a schematic model was proposed to describe the promotion of cardiac differentiation of BASCs by CNTs through the β1 integrin-dependent TGF-β1 signaling pathway (Figure 8). CNTs activated β1-integrin residing in the cytomembrane to release the active TGF-β1. Consequently, TGF-β1 mediates the activation of p-Smad2, which further stimulates the cardiac-specific transcription factors, and ultimately contributes to the facilitative effect of CNTs on BASC cardiogenesis.

Discussion

Our work established the important facilitative effects of CNTs on cardiac differentiation of BASCs and revealed the

regulating role of CNTs on structural and functional maturation of BASC-CMs by a β1 integrin-dependent TGF-β1 signaling pathway. These results suggest that the incorporation of CNTs into the native matrix represents an efficient approach to regulate cardiac differentiation of BASCs. The CNTs-based tissue-engineered platform here can not only facilitate the mechanistic understanding of molecular events initiating cardiac differentiation of stem cells but also offers a potentially safer source for cardiac regenerative medicine.

Many reports have focused on the effects of CNTs on cardiogenesis in various stem cells, such as mesenchymal stem cells and embryonic stem cells. More recently, carbon nanomaterials such as CNT and graphene have been demonstrated to favor the attachment and cardiomyogenic differentiation of mesenchymal stem cells.[30–32] In addition,

Figure 8 A schematic model was proposed to describe the promotion of cardiac differentiation of BASCs by CNTs through the β1 integrin-dependent TGF-β1 signaling pathway.
Notes: CNTs activated β1-integrin residing in the cytomembrane to release the active TGF-β1. Consequently, TGF-β1 mediates the activation of p-Smad2, which further stimulates the cardiac-specific transcription factors, and ultimately contributes to the facilitative effect of CNTs on BASC cardiogenesis.
Abbreviations: CNT, carbon nanotube; Col, collagen; BASCs, brown adipose-derived stem cells.

BASCs as potential source for cardiac regeneration were used to study the differentiation toward CMs, metabolic activity, and tissue engineering.[10–12] Although BASCs have the capability of spontaneous differentiation toward CMs, because of the naturally low efficacy it remains critical to develop novel effective strategies to promote cardiogenesis in stem cells. In this study, we showed that CNTs improved the attachment, proliferation, and cardiogenesis of BASCs. One of the possible reasons is the increased nanoroughness of substrates due to the supplementation of CNTs in Col substrates, as shown in our previous study.[19] Growth factors are the most common approach to stimulate stem cells to differentiate toward CMs, but this process is typically very expensive with limited efficiency in stimulation of specific cell lineage differentiation.[33,34] CNT-Col substrates remarkably improved and accelerated the cardiogenesis in BASCs in the absence of any chemical inducer. In contrast to exogenous chemical inducers for stem cell differentiation, this approach

is simple, inexpensive, and easy to fabricate. The data here show that the efficiency of cardiogenesis in stem cells can be increased by the simple and efficient incorporation of CNTs into substrates.

Directing stem cell differentiation into the cardiac lineages with mature functions is important for treating ischemic heart diseases and for drug screening in vitro. However, to date, there exist few efficient methods for accelerating the maturation of stem cell-derived CMs. In our study, the incorporation of CNT-Col substrates significantly promoted the maturation of BASC-CMs with better sarcomeric organization and more gap junctions, when compared to those on control substrates. With these mature functional microstructures, BASC-CMs correspondingly increased the contractile activity. Recently, nanocomposite scaffolds composed of conductive nanowires were confirmed to enhance the maturation of CMs derived from stem cells with a significantly improved sarcomere length and Z-line width.[21] Besides the

increased sarcomere length, gap junctions involved in the propagation of cardiac action potentials were another piece of evidence indicating the maturation of CMs derived from stem cells. Various conductive nanomaterials including CNTs have been reported to enhance the assembly of gap junctions between neighboring CMs to increase their impulse conduction.[26,27,35,36] Our data here also convincingly demonstrate that CNTs enhance the maturation of CMs with higher sarcomere length and greater assembly of gap junctions between adjacent CMs derived from BASCs.

Dissecting the molecular pathways involved in the differentiation and maturation of CMs derived from BASCs is critical for understanding tissue formation in the embryo and for using stem cells to regenerate the damaged myocardium. Here, we provide the evidence that CNT-Col substrates stimulate the cardiac differentiation of BASCs by activating the TGF-β1 signaling pathway. TGF-β family members, such as TGF-β1 and BMP, are reported to play important roles in stimulating the expression of cardiac-specific protein.[29,37,38] TGF-β1 exerts an essential impact in the cardiomyogenic differentiation of c-kit+ bone marrow cells by binding to two types of receptor, TβR I and TβR II, and induces the phosphorylation of Smad 2 and 3.[39,40] Consistent with these previous reports, the activation of TGF-β1 was found to be required for the CNT-induced promotion of cardiogenesis in BASCs in this study.

One striking finding was that the facilitative effect of CNTs on cardiac differentiation of BASCs is mediated by the activation of β1-integrin and triggering TGF-β1 signaling pathway. β1-integrin is the main β subunit in the heart and acts as a critical mechanotransducer, transmitting physical stress signals from the extracellular matrix into the cell.[41,42] Results have demonstrated that β1-integrin is a main sensor that affects the cardiac specification and differentiation of stem cells in the heart.[43,44] Our recent study shows that the β1-integrin-mediated signaling pathway modulates the enhanced assembly of electrical and mechanical junctions in cultured CMs due to CNTs.[19] Here, we demonstrate that the enhanced cardiac differentiation of BASCs by CNTs can be eliminated by inactivation of the TGF-β1 signaling pathway using an anti-β1-integrin neutralizing antibody. This suggests that the facilitative effect of CNTs on cardiac differentiation of BASCs is modulated by β1-integrin dependent TGF-β1 signaling pathway.

Conclusion

In summary, this study demonstrates that the incorporation of CNT-Col substrates significantly improved the cardiac differentiation efficiency of BASCs through β1-integrin-dependent TGF-β1 signaling pathway. Our study here reveals the underlying signaling pathway in the regulation of differentiation of stem cells by CNTs, which may be targeted for more effective cardiomyogenesis and thereby allow stem cells to be used more effectively in cardiac therapies.

Acknowledgments

Author contributions

Fuzhou Tian, Lijun Tang, and Hongyu Sun conceived the project and designed the experiments. Yongchao Mou, Yi Li, and Xia Li synthesized and characterized the materials. Yongchao Mou, Xia Li, performed the experiments of isolation, cultivation, and characterization of stem cells. Hongyu Sun, Yi Li, and Xia Li performed all the other experiments. Kayla Duval, Zhu Huang, and Ruiwu Dai performed all the statistical analysis. Fuzhou Tian, Hongyu Sun, Zi Chen, and Yongchao Mou cowrote the manuscript draft. All authors contributed toward data analysis, drafting and critically revising the paper and agree to be accountable for all aspects of the work.

Disclosure

The authors report no conflicts of interest in this work.

References

1. Mozaffarian D, Benjamin EJ, Go AS, et al. Heart disease and stroke statistics-2016 update: a report from the American Heart Association. *Circulation*. 2016;133:e38–e360.
2. Poole JE, Johnson GW, Hellkamp AS, et al. Prognostic importance of defibrillator shocks in patients with heart failure. *N Engl J Med*. 2008; 359:1009–1017.
3. Laflamme MA, Zbinden S, Epstein SE, Murry CE. Cell-based therapy for myocardial ischemia and infarction: pathophysiological mechanisms. *Annu Rev Pathol*. 2007;2:307–339.
4. Ptaszek LM, Mansour M, Ruskin JN, Chein KR. Towards regenerative therapy for cardiac disease. *Lancet*. 2012;379:933–942.
5. Mangi A, Noiseux N, Kong D, et al. Mesenchymalstem cells modified with Akt prevent remodeling and restore performance of infarcted hearts. *Nat Med*. 2003;9:1195–1201.
6. Ravichandran R, Venugopal JR, Mueller M, et al. Buckled structures and 5-azacytidine enhance cardiogenic differentiation of adipose-derived stem cells. *Nanomedicine (Lond)*. 2013;8:1985–1997.
7. Schlechta B, Wiedemann D, Kittinger C, et al. Ex-vivo expanded umbilicalcord blood stem cells retain capacity for myocardial regeneration. *Circ J*. 2010;74:188–194.

8. Beltrami AP, Barlucchi L, Torella D, et al. Adult cardiac stem cells are multipotent and support myocardial regeneration. *Cell*. 2003;114: 763–776.

9. Psaltis PJ, Zannettino AC, Worthley SG, et al. Concise review: mesenchymal stromal cells: potential for cardiovascular repair. *Stem Cells*. 2008;26:2201–2210.

10. Yamada Y, Wang XD, Yokoyama S, Fukuda N, Takakura N. Cardiac progenitor cells in brown adipose tissue repaired damaged myocardium. *Biochem Biophys Res Commun*. 2006;342:662–670.

11. Leobon B, Roncalli J, Joffre C, et al. Adipose derived cardiomyogenic cells: in vitro expansion and functional improvement in a mouse model of myocardial infarction. *Cardiovasc Res*. 2009;83:757–767.

12. Liu Z, Wang H, Zhang Y, et al. Efficient isolation of cardiac stem cells from brown adipose. *J Biomed Biotechnol*. 2010;2010:104296.

13. Dalby M, Gadegaard N, Tare R, et al. The control of human mesenchymal cell differentiation using nanoscale symmetry and disorder. *Nat Mater*. 2007;6:997–1003.

14. Oh S, Brammer K, Li Y, et al. Stem cell fate dictated solely by altered nanotube dimension. *Proc Natl Acad Sci U S A*. 2009;106: 2130–2135.

15. Dai H. Carbon nanotubes: synthesis, integration, and properties. *Acc Chem Res*. 2002;35:1035–1044.

16. Motta M, Li YL, Kinloch I, et al. Mechanical properties of continuously spun fibers of carbon nanotubes. *Nano Lett*. 2005;5:1529–1533.

17. Tay CY, Gu H, Leong WS, et al. Cellular behavior of human mesenchymal stem cells cultured on single-walled carbon nanotube film. *Carbon*. 2010;48:1095–1104.

18. Crowder SW, Liang Y, Rath R, et al. Poly(ε-caprolactone)-carbon nanotube composite scaffolds for enhanced cardiac differentiation of human mesenchymal stem cells. *Nanomedicine (Lond)*. 2013;8:1763–1776.

19. Sun H, Lü S, Jiang XX, et al. Carbon nanotubes enhance intercalated disc assembly in cardiacmyocytes via the b1-integrin-mediated signaling pathway. *Biomaterials*. 2015;55:84–95.

20. Dvir T, Levy O, Shachar M, Granot Y, Cohen S. Activation of the ERK1/2 cascade via pulsatile interstitial fluid flow promotes cardiac tissue assembly. *Tissue Eng*. 2007;13:2185–2193.

21. Tan Y, Richards D, Xu R, et al. Silicon nanowire-induced maturation of cardiomyocytes derived from human induced pluripotent stem cells. *Nano Lett*. 2015;15(5):2765–2772.

22. Schultz JF, Armant DR. Beta 1- and beta 3-class integrins mediate fibronectin binding activity at the surface of developing mouse peri-implantation blastocysts. Regulation by ligand-induced mobilization of stored receptor. *J Biol Chem*. 1995;270(19):11522–11531.

23. Goumans MJ, de Boer TP, Smits AM, et al. TGF-beta1 induces efficient differentiation of human cardiomyocyte progenitor cells into functional cardiomyocytes in vitro. *Stem Cell Res*. 2007;1(2):138–149.

24. Kim RY, Robertson EJ, Solloway MJ. Bmp6 and Bmp7 are required for cushion formation and septation in the developing mouse heart. *Dev Biol*. 2001;235:449–466.

25. Lian X, Hsiao C, Wilson G, et al. Robust cardiomyocyte differentiation from human pluripotent stem cells via temporal modulation of canonical Wnt signaling. *Proc Natl Acad Sci U S A*. 2012;109(27): E1848–E1857.

26. Shin SR, Jung SM, Zalabany M, et al. Carbon-nanotube-embedded hydrogel sheets for engineering cardiac constructs and bioactuators. *ACS Nano*. 2013;7:2369–2380.

27. Zhou J, Chen J, Sun H, et al. Engineering the heart: evaluation of conductive nanomaterials for improving implant integration and cardiac function. *Sci Rep*. 2014;4:3733.

28. Dvir T, Timko BP, Kohane DS, Langer R. Nanotechnological strategies for engineering complex tissues. *Nat Nanotechnol*. 2011;6:13–22.

29. TenDijke P, Arthur HM. Extracellular control of TGFbeta signalling invascular development and disease. *Nat Rev Mol Cell Biol*. 2007;8:857–869.

30. Meng X, Stout DA, Sun L, Beingessner RL, Fenniri H, Webster TJ. Novel injectable biomimetic hydrogels with carbon nanofibers and self-assembled rosette nanotubes for myocardial applications. *J Biomed Mater Res A*. 2012;101(4):1095–1102.

31. Mooney E, Mackle JN, Blond DJ, et al. The electrical stimulation of carbon nanotubes to provide a cardiomimetic cue to MSCs. *Biomaterials*. 2012;33(26):6132–6139.

32. Park J, Park S, Ryu S, et al. Graphene-regulated cardiomyogenic differentiation process of mesenchymal stem cells by enhancing the expression of extracellular matrix proteins and cell signaling molecules. *Adv Healthc Mater*. 2014;3(2):176–181.

33. Reinecke H, Minami E, Zhu WZ, Laflamme MA. Cardiogenic differentiation and transdifferentiation of progenitor cells. *Circ Res*. 2008;103(10): 1058–1071.

34. Karantalis V, Hare JM2. Use of mesenchymal stem cells for therapy of cardiac disease. *Circ Res*. 2015;116(8):1413–1430.

35. Dvir T, Timko BP, Brigham MD, et al. Nanowired three-dimensional cardiac patches. *Nat Nanotechnol*. 2011;6:720–725.

36. Martinelli V, Cellot G, Toma FM, et al. Carbon nanotubes promote growth and spontaneous electrical activity in cultured cardiac myocytes. *Nano Lett*. 2012;12:1831–1838.

37. Behfar A, Zingman LV, Hodgson DM, et al. Stem cell differentiation requires a paracrine pathway in the heart. *FASEB J*. 2002;16: 1558–1566.

38. Slager HG, Van Inzen W, Freund E, et al. Transforming growth factor-beta in the early mouse embryo: implications for the regulation of muscle formation and implantation. *Dev Genet*. 1993;14:212–224.

39. Lagostena L, Avitabile D, De Falco E, et al. Electrophysiological properties of mouse bone marrow c-kit+ cells co-cultured onto neonatal cardiac myocytes. *Cardiovasc Res*. 2005;66:482–492.

40. Shi M, Zhu J, Wang R, et al. Latent TGF-β structure and activation. *Nature*. 2011;474:343–349.

41. Israeli-Rosenberg S, Manso AM, Okada H, et al. Integrins and integrin-associated proteins in the cardiac myocyte. *Circ Res*. 2014;114: 572–586.

42. Schwartz MA. Integrins and extracellular matrix in mechanotransduction. *Cold Spring HarbPerspect Biol*. 2010;2:a005066.

43. Rohwedel J, Guan K, Zuschratter W, et al. Loss of beta1 integrin function results in a retardation of myogenic, but an acceleration of neuronal, differentiation of embryonicstem cells in vitro. *Dev Biol*. 1998;201: 167–184.

44. Zeng D, Ou DB, Wei T, et al. Collagen/β(1) integrin interaction is required for embryoid body formation during cardiogenesis from murine induced pluripotent stem cells. *BMC Cell Biol*. 2013;14:5.

Supplementary materials

Table S1 Primers used in the RT-PCR studies

Name	Sense	Antisense
Nkx2.5	5′ ACCATGCGGGAAGGCTAT 3′	5′CTCCAGGTTCAGGATGTCTTTG 3′
GATA-4	5′ CTGTCATCTCACTATGGGCA 3′	5′ TTAAGGACGAGCCTGAACC 3′
Tbx5	5′ TGACTGGCCTTAATCCCAAA 3′	5′ ACAAGTTGTCGCATCCAGTG 3′
α-MHC	5′ CAAGACTGTCCGGAATGACA 3′	5′ GGCTTCTTGTTGGACAGGAT 3′
β-MHC	5′ ATGTGCCGGACCTTGGAAG 3′	5′ CCTCGGGTTAGCTGAGAGATCA 3′
cTnT	5′ CTCGGAGTATCAGGAAGAGCACA 3′	5′ GATACTGGACGCACCGTTCAAA 3′
GAPDH	5′ GCAAGTTCAACGGCACAG 3′	5′ GCCAGTAGACTCCACGACAT 3′

Abbreviation: RT-PCR, real-time reverse transcription-polymerase chain reaction.

Video S1 Light microscopy of the BASCs on the Col substrate at day 7.

Video S2 Light microscopy of synchronously contracted BASCs on the CNT-Col substrate at day 7.